



Journal of Materials and Engineering Structures

Research Paper

A pile-up of edge dislocations to relax Misfit strain

Aziz Soufi^a, Ayoub Aitoubba^b, Khalil El-Hami^{c,*}, Mohamed Talea^b, Assia Bakali^b, Jean Grilhé^d

^a University of Hassan 1st, National School of Applied Sciences, Laboratory of Nanosciences and Modeling, Khouribga, Morocco

^b University of Hassan II, Faculty of Sciences Ben M'sik, Information Processing Laboratory, Casablanca, Morocco

^c University of Hassan 1st, Faculty of Khouribga, Laboratory of Nanosciences and Modeling, Khouribga, Morocco

^d University of Poitiers, Sciences Institut Bprime Condensed Matter Physics and Materials Physics, Poitiers, France

ARTICLE INFO

Article history :

Received : 28 December 2016

Accepted : 29 January 2017

Keywords:

Thin film

Heteroepitaxial growth

Misfit Strain

Misfit dislocation

ABSTRACT

It is shown that very large stresses may be present in the thin films that comprise integrated circuits and magnetic disks and that these stresses can cause deformation and fracture of the material. For a crystalline film on a non-deformable substrate, a key problem involves the movement of dislocations in the thin film. An analysis of this problem provides insight into both the formation of misfit dislocations in epitaxial thin films and the high strengths of thin metal films on substrates. We develop in this paper, theoretical calculations for dislocation nucleation phenomena in nanomaterials obtained by hetero-epitaxial growth of thin films on substrates having lattice mismatch defects. Atomic force microscopy observations showed the nucleation of dislocations from free lateral surfaces to relax the "misfit" strain, here we explain the principle of nucleating edge dislocations from these surfaces by the theoretical calculation, using the method of image stress and energy study. We begin, by treating the case of a single dislocation and then generalize the work at a pile-up of n interface dislocations.

1 Introduction

The technical of thin-film deposits by various methods such as the hetero-epitaxial technique in the nanoscale level, have become the process of obtaining the best materials in various application areas as diverse as ferroelectric materials, optics materials with reflective layers and electric field with the metallic conductive layers... Plastic deformation of crystalline materials is often associated to the mobility of dislocations [1-7], see (Fig.1) [8]. In contrast, the ductility is maintained as dislocations have good mobility; the material is then deformed conserving the unit of its structure.

* Corresponding author. Tel.: +212673638424

E-mail address: khalil.elhami@uhp.ac.ma

e-ISSN: 2170-127X,

Transmission electron microscopy of hetero-structures has enabled the onset and subsequent development of misfit dislocations to be followed for increasing strained-layer thicknesses. A well-known mechanism is that of Frank-Read [9; 10; 11] by which a dislocation pinned at its two ends gives rise to numerous dislocation loops. In nanostructured materials, the reduced dimensions make the dislocation sources of activation more unlikely, often the number of pre-existing dislocations is also very low, so this is a very challenging problem, because the relaxation mechanism involves nucleation and motion of threading dislocations through the thin film. Plasticity works by the formation of new dislocations from particular sites such as crack fronts, precipitates, interfaces, or surface defects. The surfaces have a special role because they are present for any size of the sample studied. Multiple experimental methods are used to study the formation of dislocations from the free surfaces, but experience encounter major difficulties in studying the earliest stages of plasticity at the atomic scale and with sufficient time resolution. Elastic theory, which describes the dislocations as linear defects moving in a continuous medium, allowed a first approach to solve this ambiguity. The modes of the most observed plasticity are irreversible deformation induced by nucleation, multiplication and dislocation motion. These movements can be glides (conservative shear) or mounted (non-conservative)[1-7].In bulk materials, one of the known mechanisms of multiplication of dislocations is Frank-Read process [9-11].In nanostructures materials free of dislocations, no source of Frank-Read can not be created, recent experimental observations showed that the plasticity operates differently : stress relaxation dislocations are nucleated from particular sites such as grain boundaries, cracks fronts, precipitates, interfaces, defects and surface irregularities such as steps [12], terraces, islands etc...See (Fig.2) [12].

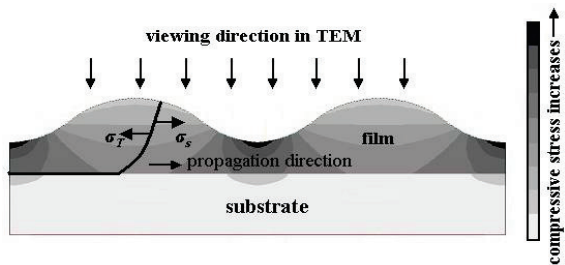


Fig.1 – Schematic diagram showing the stress fields experienced by a propagating dislocation cutting

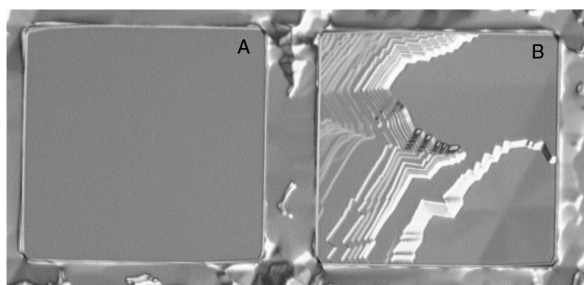


Fig. 2 – DIC optical micrographs of two 200 μm x 200 μm mesas following homoepitaxial growth. Mesa (a) formed a step - free surface, mesa (b) bunched steps and a hexagonal growth

Nucleation of dislocations from surfaces and interfaces is an important process in the plastic deformation of the stress at the nanoscale materials. Among these nucleating sources defects surfaces have very specific roles, they are present in the bulk samples and nanostructures (as nano grains, whiskers and multilayer). The surfaces also play a large role in the plastic deformation of thin films [13-15]. For lattice mismatched epitaxial layers, the thin film is subjected to stresses in compression or tension and it is widely accepted that there exists a critical thickness beyond which misfit dislocations are introduced causing the breakdown of coherence between the substrate and epitaxial layers. This is called misfit stresses [16, 17]. The critical thickness is defined as the thickness at which the first misfit dislocation nucleates. The energy of the system due to the elastic deformation increases as the thickness of the thin film increases [18]. When the stored energy becomes greater than the activation energy of a dislocation, it is nucleated from the free surface and slides up the interface (Fig.3) [19].

They are called epitaxial growth dislocations and adjust the incoherence of crystal lattices. In this context and following the failure of all experimental information about the early stages of nucleation (resolution electron microscopy limit), we used the theoretical model based on the energy study [18, 24–27] about the behaviour of a dislocation nucleated near of a free lateral surface to generalize a pile up of n dislocations issued by the same nucleation method.

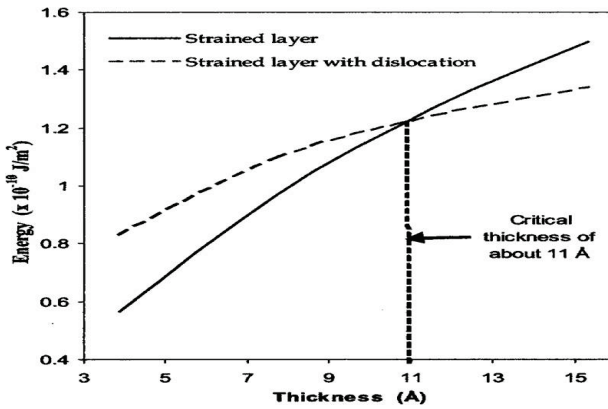


Fig.3 – Calculation of the critical thickness for the Co/Cu system by FEM simulation of growth of the film and a dislocation.

2 Interaction between Two Parallel Edge Dislocations

The first edge dislocation in position $(0, 0, z)$, acting as the source of the stress field “Fig.4”. It has the z-axis as line of dislocation. The second edge dislocation may be in an arbitrary position, but parallel to the first. The Burgers vectors of the two dislocations are assumed to be equal. We consider the case of the second dislocation being able to glide on a plane parallel to the xy-plane, but not to climb. Hence, the force on the second dislocation has to point in the x-direction and, according to the Peach and Koehler formula [2] it is produced by the shear stress component σ_{xy} .

$$dF = |\mathbf{b}|[\sigma_b \times d\mathbf{l}] \quad \text{Peach and Koehler formula} \quad (1)$$

with

\mathbf{b} : Burgers vector,

$d\mathbf{l}$: vector element in the direction of the dislocation line,

σ_b : stress on the plane normal to the Burgers vector, and on which \mathbf{b} points outwards.

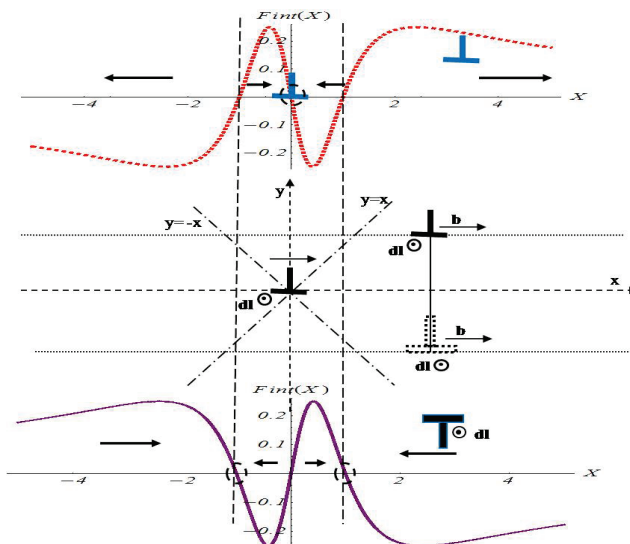


Fig.4 – Force between two parallel edge dislocations, under the condition that only glide is permitted. (The circles mark stable positions)

According to the Peach and Koehler formula, the force on the second dislocation is:

$$\left\{ \begin{array}{l} \vec{F}_x = \frac{\mu \cdot b_1 \cdot b_2}{2 \cdot \pi \cdot (1-v)} \cdot \frac{x \cdot (x^2 - y^2)}{(x^2 + y^2)^2} \vec{e}_x \\ b_1 = b \\ b_2 = \pm b \end{array} \right. \quad (2)$$

$$\left\{ \begin{array}{l} \mu = \text{shear modulus} \\ v = \text{Poisson's ratio} = 1/3 \end{array} \right.$$

$$\left\{ \begin{array}{l} F_x = -\frac{\partial}{\partial x} (W_{int}) \\ \frac{\partial^2}{\partial x^2} (W_{int}) = -\frac{\partial}{\partial x} (F_x) = \frac{-\mu \cdot b_1 \cdot b_2}{2 \cdot \pi \cdot (1-v)} \cdot \left(-\frac{4x^2(x^2 - y^2)}{(x^2 + y^2)^3} + \frac{2x^2}{(x^2 + y^2)^2} + \frac{x^2 - y^2}{(x^2 + y^2)^2} \right) \end{array} \right. \quad (3)$$

An equilibrium situation:

$$\left\{ \begin{array}{l} \frac{\partial}{\partial x} (W_{int}) = 0 \\ \frac{\partial^2}{\partial x^2} (W_{int}) \geq 0 \text{ stable situation} \\ \frac{\partial^2}{\partial x^2} (W_{int}) \leq 0 \text{ unstable situation} \end{array} \right.$$

For two equal parallel edge dislocations there is a stable situation for glide at $x = 0$:

$$\left\{ \begin{array}{l} x = 0 \\ \frac{\partial}{\partial x} (W_{int}) = 0 \\ \frac{\partial^2}{\partial x^2} (W_{int}) = \frac{-\mu \cdot b_1 \cdot b_2}{2 \cdot \pi \cdot (1-v)} \cdot \left(\frac{-1}{y^2} \right) \geq 0 \\ b_1 = b_2 = b \end{array} \right.$$

And of two edge dislocations with opposite signs stable situations also exist, but here they appear for $|x| = |y|$:

$$\left\{ \begin{array}{l} x = \pm y \\ \frac{\partial}{\partial x} (W_{int}) = 0 \\ \frac{\partial^2}{\partial x^2} (W_{int}) = \frac{-\mu \cdot b_1 \cdot b_2}{4 \cdot \pi \cdot (1-v)} \cdot \left(\frac{1}{y^2} \right) \geq 0 \\ b_1 = -b_2 = b \end{array} \right.$$

The physical reason for the stability of the arrangement of two dislocations placed on top of each other lies in the fact that they form part of a possible interface between two crystals, slightly tilted with respect to one another

3 The first nucleated dislocation

3.1 Stresses and forces acting on the dislocation

Consider a semi infinite solid delimited by a free surface $x = 0$ and located on the side negative x . This solid contains a buried epitaxial film between $y = h$ and $y = -h$ (Fig. 5). Epitaxial stresses are calculated from distributions of dislocations interfaces, characterized by Burgers vectors $\vec{b} = \pm \vec{\delta a}$ ($+\delta a$ in the plane $y = h$ and $-\delta a$ in the plane $y = -h$) with a density $\frac{dx}{a}$, "a" is the lattice parameter

One edge dislocation of Burgers vector $(b, 0)$ is introduced from the free lateral surface ($x = 0, y$), concerned interface: $y = h$. The sign of b being opposite the sign of δa .

We have determined total stress, total force and the total energy of edge dislocation studied

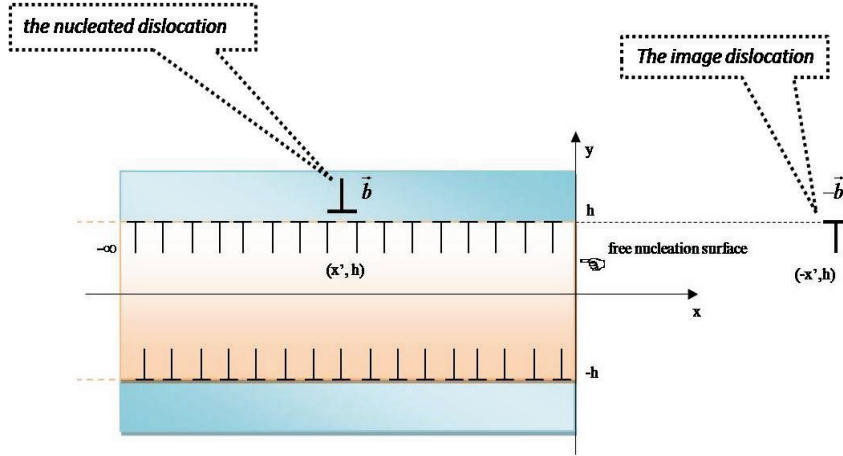


Fig.5– The effect of epitaxial shear stress and Image stress illustration

- The Image stress:

Modeled as shown in (Fig.5) it is annulling the direct effect of the studied dislocation (x' , h) at the free surface (modeling the attractive force). Using The field of shear stress created by the dislocation located in origin (0,0) at a point (x , y) in an infinite space[2; 3] given by :

$$\left\{ \begin{array}{l} \tau_{xy} = \frac{\mu.b}{2.\pi.(1-\nu)} \cdot \frac{x.(x^2-y^2)}{(x^2+y^2)^2} = \frac{-\partial^2}{\partial x \partial y} \psi(x,y) \\ \psi(x,y) = -D.y \ln \sqrt{x^2 + y^2} \text{ the Airy fonction} \\ D = \frac{\mu.b}{2.\pi.(1-\nu)} \end{array} \right. \quad (4)$$

So, we have:

$$\sigma^{\text{image}} = \frac{-\mu.b}{4.\pi.(1-\nu).x} \quad (5)$$

- The epitaxial Stress

The Epitaxial stress calculation at the dislocation nucleation (x ; y) was done by summing of $-\infty$ to 0 the effects of:

- The direct action of the dislocation distribution at the interface $y = +h$
- The direct action of the dislocation distribution at the interface $y = -h$
- and respectively, the effect of their images stresses.

Using the formal calculation code Mathematica, and after simplification it has been demonstrated:

$$\sigma_{xy}^{\text{epit}} = \frac{\mu.b}{2.a.\pi.(1-\nu)} \cdot \left[\frac{4.x^2}{x^2+(y-h)^2} - \frac{4.x^2}{x^2+(y+h)^2} \right] \quad (6)$$

So for $y=h$, the total stress one dislocation considered is:

$$\sigma_{xy}^{\text{tot}}(x, h) = \frac{-\mu.b}{4.\pi.(1-\nu).x} + \frac{4.\mu.b}{2.a.\pi.(1-\nu)} \cdot \left[1 - \frac{x^2}{x^2+4.h^2} \right] \quad (7)$$

- And The total force

Is given by the formula Peach and Koehler [2; 3]:

$$\left\{ \begin{array}{l} \overrightarrow{f_{epit}} + \overrightarrow{f_{image}} = \overrightarrow{f_{tot}} = \frac{4.\mu.b}{2.\pi.(1-\nu)} \cdot \epsilon^{epit} \left(1 - \frac{x^2}{x^2+4.h^2} \right) \vec{e}_x + \frac{-\mu.b^2}{4.\pi.(1-\nu).x} \vec{e}_x \\ \xi: \text{line vector} \\ \epsilon^{epit} = \frac{\delta a}{a} \end{array} \right. \quad (8)$$

3.2 The total force and energy of dislocation acting on the dislocation

3.2.1 Theoretical calculations

For a very simple study, reduced coordinates are used:

$$\left\{ \begin{array}{l} X = \frac{x}{2.h}; B = \frac{b}{2.h} \\ k = \frac{\epsilon^{epit}}{B} < 0 \\ F = \frac{f \cdot 2.\pi.(1-\nu)}{2.\mu.h.B^2} \end{array} \right.$$

We get:

$$\left\{ \begin{array}{l} F_{im} = \frac{-1}{2.X} > 0 \\ F_{epit} = \frac{4.k}{X^2+1} < 0 \\ F_{tot} = \frac{4.k}{X^2+1} - \frac{1}{2.X} \end{array} \right.$$

Then, the total work force when the dislocation moves from x_0 to x (x_0 radius of the dislocation core), was obtained by:

$$\left\{ \begin{array}{l} W(x) = - \int_{x_0}^x (F_{im}(X') + F_{epit}(X')) . dX' \\ W(X) = \frac{1}{2} \cdot \text{Log} \left(\frac{X}{X_0} \right) - 4.k \cdot (\text{Arctg}(X) - \text{Arctg}(X_0)) \end{array} \right. \quad (9)$$

3.2.2 Graphical representation of the energy function

On the graphs (Fig. 6) are shown respectively the energy for $k = -0.7$ (6.a) and for different values of k (6.b).

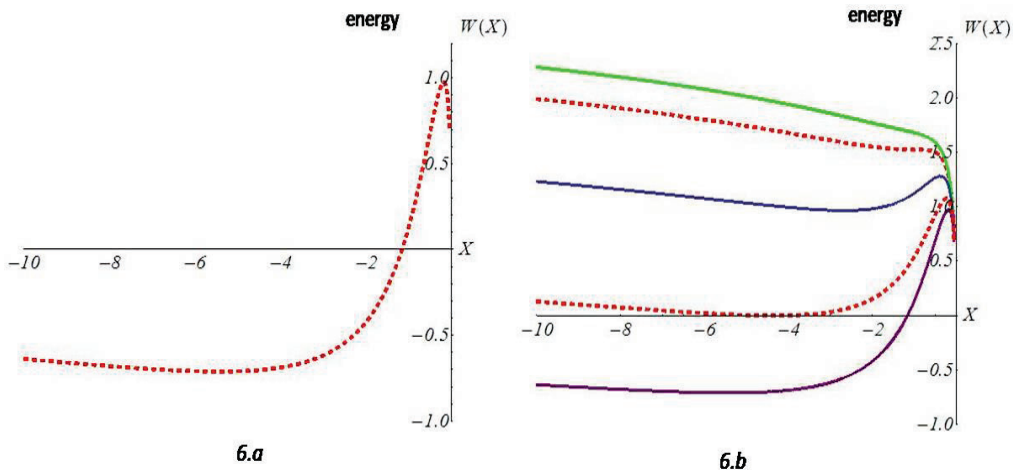


Fig.6– energy variation following the variation of the strain epitaxial growth

The equilibrium positions are given by:

$$F_{tot}(X) = \frac{4 \cdot k}{X^2 + 1} - \frac{1}{2 \cdot X} = 0$$

- For $k > k_{c1} = \frac{-1}{4}$ no equilibrium position, this is when the thickness h of buried thin film is too low:

$$k = \frac{\delta a}{a} \cdot \frac{b}{2 \cdot h} > \frac{-1}{4}$$

- For $k < k_{c1} = \frac{-1}{4}$ there are two equilibrium positions:

The first is stable: $X_{st} = 4 \cdot k - \sqrt{16 \cdot k^2 - 1}$ And the other unstable: $X_{inst} = 4 \cdot k + \sqrt{16 \cdot k^2 - 1}$

3.3 Conclusion

From the curves of the two graphs, one can deduce:

- Fig.6.a: the reduced energy graph has a Minimum which represents a stable equilibrium position; therefore we can control the nucleation of dislocation to accommodate and to relax the lattice mismatch between a heteroepitaxial thin film and its substrate. An equilibrium position which depends on k , ie which the strain epitaxial growth δa and the thickness h of the deposited thin film.

- Fig.6.b: The group of four curves shows and confirmed analytically and theoretically the result noted in the first remark: $k = k_{c1} = \frac{-1}{4}$ critical case ($\Delta = 0$) from which when $k > k_{c1} = \frac{-1}{4}$ (green curve) no equilibrium position is possible, so we can not relax the lattice mismatch strain by nucleation of dislocation from the free surface.

- For $k_{c2} = -0.529 \leq k \leq \frac{-1}{4}$ (blue curve) in the middle shows a position of equilibrium which is metastable and outside the material, so impossible to accommodate the incoherence of epitaxial defect.

- For $k = k_{c2} = -0.529$ (dashed red curve below), it is the lower limit of the critical area value (the curve is tangent to the $y = 0$), then we will always be in the metastable zone.

- For $k > k_{c2} = -0.529$, the energy of the stable equilibrium position is negative ($W(X_{st}) < 0$) and the equilibrium position is stable, that is where the nucleation of dislocation relaxes the lattice mismatch defect. These results can be shown through the graph Fig.7 (below) where we summarized the zone of stability and metastability of our dislocation depending of $\frac{\delta a}{a}$ and the film thickness h .

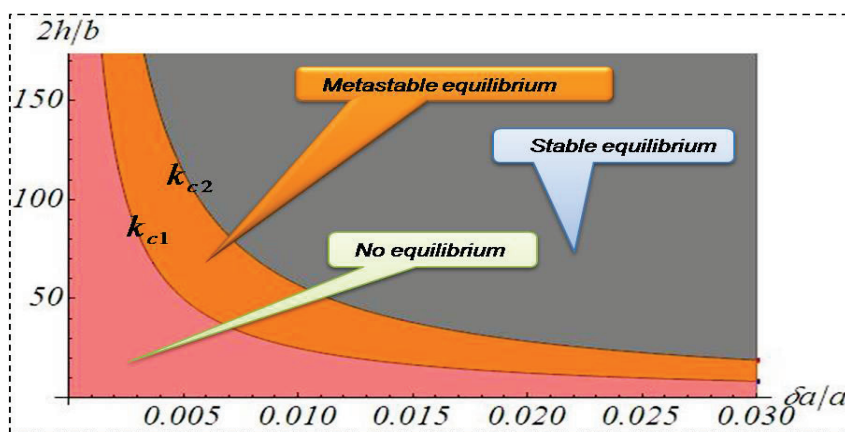


Fig. 7 – stability area, metastability and field of instability depending on $\frac{\delta a}{a}$ and the thin film thickness h

4 The pile-up of dislocations

4.1 Pair of two dislocations ($n = 2$)

We now consider a pair of two dislocations nucleated one after the other to relax the misfit strain. Burgers vector $(\mathbf{b}, 0)$ at the interface $y = h$ and respectively X_1 and X_2 .

The total force applied to the dislocation number (i):

$$F_i = f_i + f_{int}(j, i) = \frac{4.k}{X_i^2 + 1} - \frac{1}{2.X_i} + \frac{1}{X_i - X_j} - \frac{1}{X_i + X_j} + 2.X_j \cdot \frac{X_j - X_i}{(X_i + X_j)^3} \quad (10)$$

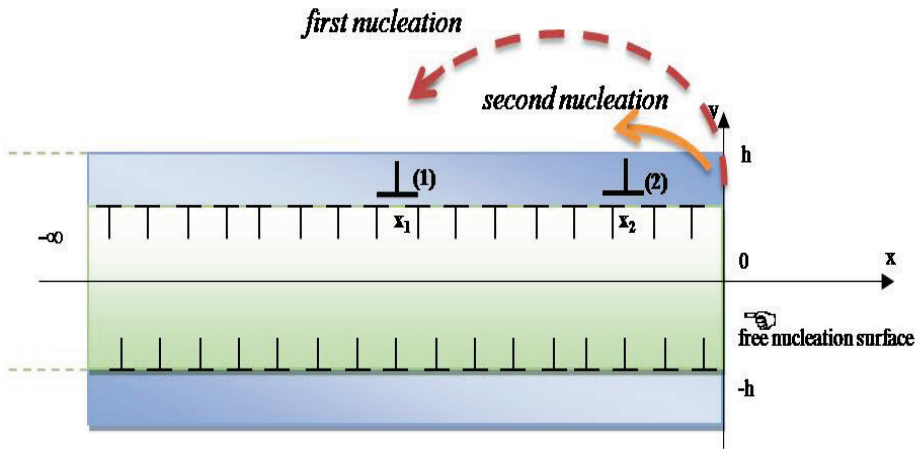


Fig.8 – introduction of two edge dislocations

So :

$$\begin{cases} F_1 = f_1 + f_{int}(2,1) = \frac{4.k}{X_1^2 + 1} - \frac{1}{2.X_1} + \frac{1}{X_1 - X_2} - \frac{1}{X_1 + X_2} + 2.X_2 \cdot \frac{X_2 - X_1}{(X_1 + X_2)^3} \\ F_2 = f_2 + f_{int}(1,2) = \frac{4.k}{X_2^2 + 1} - \frac{1}{2.X_2} + \frac{1}{X_2 - X_1} - \frac{1}{X_2 + X_1} + 2.X_1 \cdot \frac{X_1 - X_2}{(X_2 + X_1)^3} \end{cases}$$

$$\begin{cases} F_1 = 0 \\ F_2 = 0 \end{cases}$$

By solving the system:

And using the calculation code Mathematica, by varying k we calculate the equilibrium positions, X_{1eq} and X_{2eq} of the two dislocations. We group the calculation results in the following table: "Table 1"

Fig.9: shows in blue and red these X_{1eq} and X_{2eq} equilibrium positions for: " $k < k_{c2} = -0.4$ ".

The green curve represents the equilibrium position X_{0eq} for a single dislocation of Burgers vector \vec{b} . For $k \geq k_{c2}$ no equilibrium position and one of the two dislocations "nearest (2)" leaves the material.

So, this accommodation of misfit strain by a pair of two edge dislocations stops to be possible:

$(k_{c2} = -0.4)$ is the critical value from which the equilibrium is not possible, dislocation 2 exits the material and circumstances to prevent using a sufficient activation energy dependent on the strain misfit $\delta\alpha$ and the thickness h of the thin film.

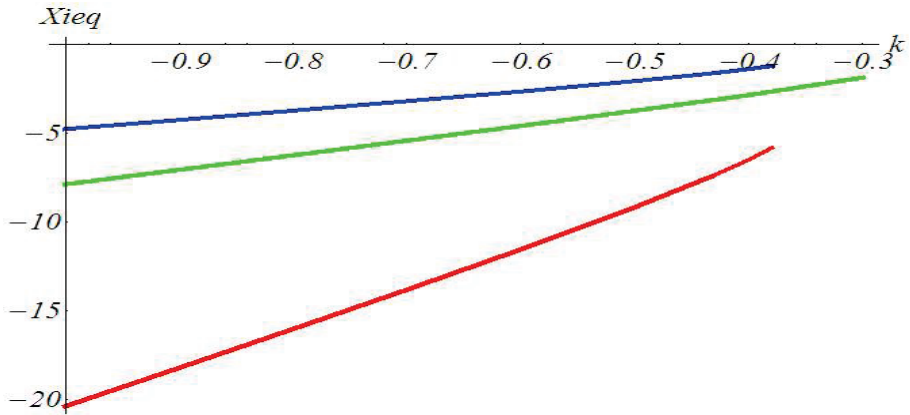


Fig. 9 – Equilibrium positions X_{1eq} (blue), X_{2eq} (red) and X_{0eq} (green)

4.2 Generalization to a pile of more than two dislocations

$n = 3$ and $n = 4$ dislocations

- F_i : Force no acting on the dislocation number (i)

$$F_i(X_i, X_j) = -\frac{1}{2.X_i} + \frac{4.k}{X_i^2+1} + \sum_{j \neq i}^n \frac{1}{X_i-X_j} - \frac{1}{X_i+X_j} + 2.X_j \cdot \frac{X_j-X_i}{(X_i+X_j)^3} \quad (11)$$

- F_j : Force acting on the dislocation number (j)

$$F_j(X_i, X_j) = -\frac{1}{2.X_j} + \frac{4.k}{X_j^2+1} + \sum_{i \neq j}^n \frac{1}{X_j-X_i} - \frac{1}{X_j+X_i} + 2.X_i \cdot \frac{X_i-X_j}{(X_j+X_i)^3} \quad (12)$$

Direct calculation of equilibrium positions X_{eq} becomes impossible. So we used the iterative conjugate gradient method:

- Cases of 3 dislocations

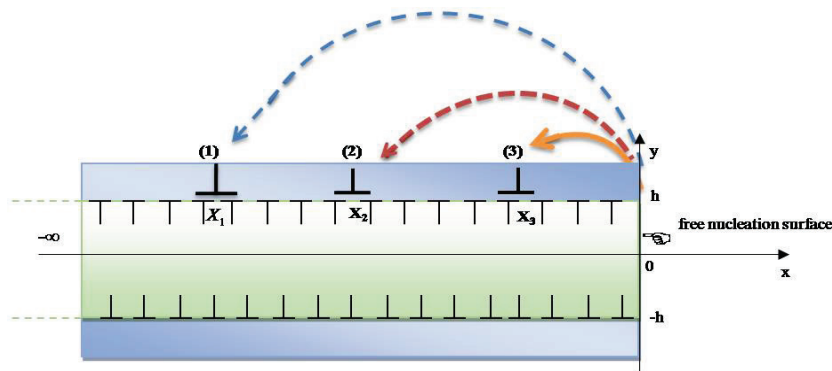


Fig.10 – introduction of 3 edge dislocations

We have initiated the calculation from the positions:

$$\begin{cases} X_{01} = -20 \\ X_{02} = -8 \\ X_{03} = -2 \\ k_0 = -1.2 \end{cases}$$

We group the results obtained in "Table2"

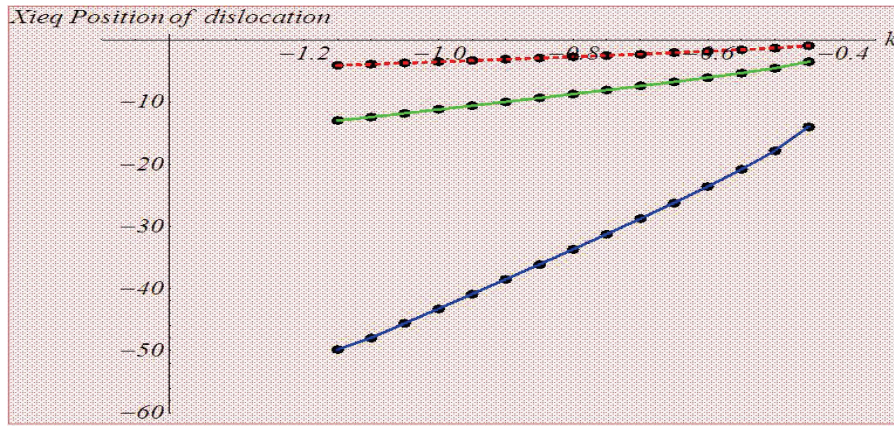


Fig.11 – stable equilibrium positions of the three dislocations

With a pile-up of 3 dislocations, we note that the stable Equilibrium stops from critical value of k ($k_{c3} = -0.45$). Dislocation Number 3, nearest the surface exits the material: *Fig. 11*.

- Cases of 4 dislocations

Always using the conjugate gradient method and for 4 dislocations, we initiated the calculation from the positions:

$$\begin{cases} X_{01} = -40 \\ X_{02} = -23 \\ X_{03} = -8 \\ X_{04} = -2 \\ k_0 = -1.3 \end{cases}$$

Results obtained: "Table3" and "Table4"

As in the case of 3 dislocations, for a pile of 4 dislocations stable equilibrium stops from the critical value of k ($k_{c4} = -0.55$). Dislocation number 4, nearest the surface exits the material: **Figure 12**.

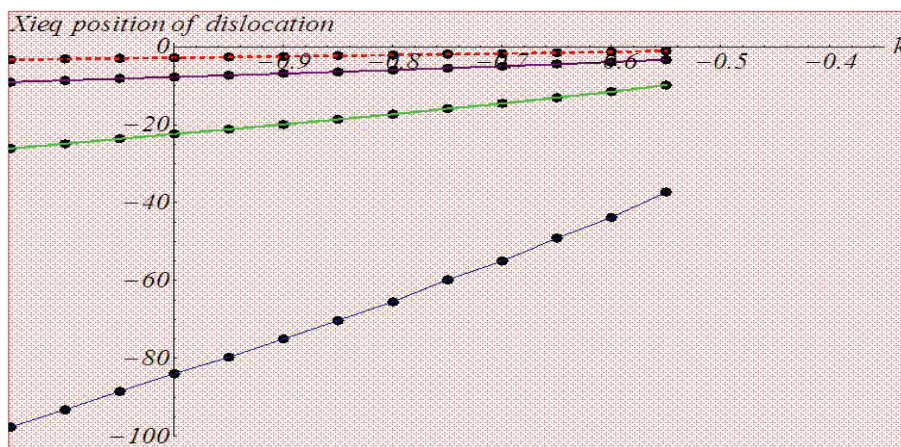


Fig.12 – Stable equilibrium positions for 4 dislocations

As was done in the case of 2 dislocations, *Fig 13*. Illustrates the zones of stability depending on the value of

$k = f(\epsilon^{epit}, h)$ for a pile-up of 4 dislocations

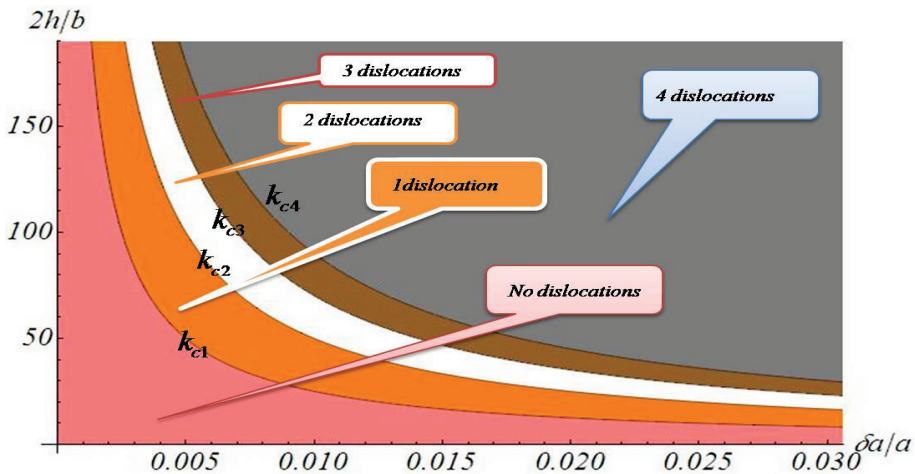


Fig. 13 – graph illustrating the curves $|k| = f\left(\frac{\delta a}{a}, h\right) = C^{te}$, stability area, metastability and field of instability

Table 1 – X_{1eq} and X_{2eq} by varying k

k	-1	-0.9	-0.8	-0.7	-0.6	-0.5	-0.43	-0.4	-0.38
X_{1eq}	-20.37	-18.21	-16.02	-13.81	-11.54	-9.17	-7.36	-6.49	-5.83
X_{2eq}	-4.76	-4.25	-3.73	-3.19	-2.65	2.06	-1.61	-1.38	-1.21
X_{0eq}	-7.87	-7.06	-6.24	-5.42	-4.58	-3.73	-3.12	-2.85	-2.66

Table 2 – X_{1eq} , X_{2eq} and X_{3eq} by varying k

k	-1.15	-1.10	-1.05	-1.00	-0.95	-0.90	-0.85	-0.80	-0.75	-0.70	-0.65	-0.60	-0.55	-0.50	-0.45	-0.40
X_{1eq}	-23.6	-22.5	-21.5	-20.4	-19.3	-18.2	-17.1	-16.0	-14.9	-13.8	-12.7	-11.5	-10.4	-9.2	-7.9	-6.5
X_{2eq}	-5.5	-5.3	-5.0	-4.8	-4.5	-4.3	-4.0	-3.7	-3.5	-3.2	-2.9	-2.6	-2.4	-2.1	-1.8	-1.4

Table 3 – 4 dislocations: X_{1eq} , X_{2eq} , X_{3eq} and X_{4eq} by varying k

k	-1.15	-1.10	-1.05	-1.00	-0.95	-0.90	-0.85	-0.80	-0.75	-0.70	-0.65
X_{1eq}	-49.20	-47.94	-45.60	-43.25	-40.88	-38.51	-36.11	-33.69	-31.24	-28.75	-26.21
X_{2eq}	-12.96	-12.41	-11.80	-11.19	-10.57	-9.95	-9.32	-8.69	-8.06	-7.41	-6.74
X_{3eq}	-4.09	-3.91	-3.72	-3.52	-3.31	-3.12	-2.91	-2.70	-2.49	-2.27	-2.06

Table 4 – X_{1eq} , X_{2eq} , X_{3eq} and X_{4eq} by varying k : Continued results table 4

k	-0.60	-0.55	-0.50	-0.45	-0.40
X_{1eq}	-23.59	-20.83	-17.83	-13.98	-13.09
X_{2eq}	-6.05	-5.33	-4.53	-3.50	-2.85
X_{3eq}	-1.82	-1.57	-1.29	-0.91	$-6.63 \cdot 10^{-11}$

5 General Conclusion

Following this work, we studied how to introduce a pileup of n dislocations ($n = 2; 3; 4\dots$) nucleated from a free lateral surface, experimentally observed at the nanometer level. The method used here, is that of the energy model and theoretical analytic calculations. The introduction of misfit dislocations is Very important and major operation, because it provides a basis for understanding the dislocation processes responsible for plastic deformation of thin films on non deformable substrates. We have shown by calculation and through the curves $k = f(\frac{\delta a}{a}, h)$ that we can control and prevent the

emergence of this pile-up of dislocations taking into consideration the misfit strain $\epsilon = \frac{\delta a}{a}$ and the effect of the thickness h of the layer, which are two parameters very significant for controlling constantly during development materials operations by deposits from thin films. There's even better and we can always do better, with a more advanced calculation again, in order to find other conditions much better about this technique of production of high-performance materials.

Note that, once again the results of the curves $k = f(\frac{\delta a}{a}, h)$ showing the areas of stability and metastability permits us to reaffirm the validity of the findings of Van der Merwe and Matthews and Blakeslee.

REFERENCES

- [1]- D. Hull, D.J. Bacon, Introduction to Dislocations, fourth ed, Butterworth Heinemann, 2001.
- [2]- J.P. Hirth, J. Lothe, Theory of dislocations. Materials Science and Engineering Series, Second edition, 1982.
- [3]- R. Hill, The mathematical theory of plasticity, Oxford Classic Texts, 1998.
- [4]- I.S. Sokolnikoff, Mathematical Theory of Elasticity, University of California, 1946.
- [5]- A.M. Kossevich, The Crystal Lattice: Phonons, Solitons, Dislocations, Wiley-VCH Verlag GmbH & Co. KGaA, Weinheim, FRG. 1999.
- [6]- S. Timoshenko, J.N. Goodier, Theory of Elasticity, New York-Toronto-London : McGraw-Hill Book Co., 1951.
- [7]- C.C. Wu, E.A. Stach, R. Hull, Nanoscale mechanisms of misfit dislocation propagation in undulated Si_{1-x}Gex/Si (100) epitaxial thin films. *Nanotechnology* 18 (2007) 165705. doi:10.1088/0957-4484/18/16/165705
- [8]- T. Shimokawa, S. Kitada, Dislocation Multiplication from the Frank-Read Source in Atomic Models, *Mater. Trans.* 55(1) (2014) 58-63. doi:10.2320/matertrans.MA201319
- [9]- F.C. Frank, W.T. Read, Jr., Multiplication Processes for Slow Moving Dislocations, *Phys. Rev.* 79(1950) 722. doi:10.1103/PhysRev.79.722
- [10]- H. H. Wang, S. Y. Byrapa, F. Wu, B. Raghethamachar, M. Dudley, E. K. Sanchez, D. M. Hansen, R. Drachev, S. G. Mueller, M. J. Loboda, Basal Plane Dislocation Multiplication via the Hopping Frank-Read Source Mechanism and Observations of Prismatic Glide in 4H-SiC. *Mater. Sci. Forum* 717-720(2012) 327-330. doi:10.4028/www.scientific.net/MSF.717-720.327
- [11]- P.G. Neudeck, J.A. Powell. Homoepitaxial and Heteroepitaxial Growth on Step-Free SiC Mesas. In: Silicon Carbide, Part II, (2004) 179-205. doi:10.1007/978-3-642-18870-1_8
- [12]- X. Wu, G.C. Weatherly, The first stage of stress relaxation in tensile strained In_{1-x}GaxAs_{1-s}Py films, *Philosophal Magazine A*. 81(6) (2001) 1489-1506. doi:10.1080/01418610108214359
- [13]- E. Le Bourhis, G. Patriarche, Deformations induced by a Vickers indentor in InP at room temperature. *Eur. Phys. J. Appl. Phys.* 12 (2000) 31-36. doi:10.1051/epjap:2000168
- [14]- L. Largeau, G. Patriarche, E. Le Bourhis, Subsurface deformations induced by a Vickers indenter in GaAs/AlGaAs superlattice, *J. Mater. Sci. Lett.* 21(5) (2002) 401-404. doi:10.1023/A:1014971619783
- [15]- J.W. Matthews, Defects associated with the accommodation of misfit between crystals, *J. Vac. Sci. Technol.* 12(1) (1975). doi:10.1116/1.568741
- [16]- W.D. Nix. Mechanical Properties of Thin Films. Stanford University, 2005.
- [17]- T. Zhu, J. Li, A. Samanta, A. Leach, K. Gall, Temperature and Strain-Rate Dependence of Surface Dislocation Nucleation, *Phys. Rev. Lett.* 100 (2008) 025502. doi:10.1103/PhysRevLett.100.025502
- [18]- A. Subramanian. Critical thickness of equilibrium epitaxial thin films using finite element method. *J. Appl. Phys.* 95(12) (2004) 8472. doi:10.1063/1.1745115
- [19]- R. Rabe, J.-M. Breguet, P. Schwaller, S. Stauss, F.-J. Haug, J. Patscheider, J. Michler, Observation of fracture and plastic deformation during indentation and scratching inside the scanning electron microscope. In: Proceedings of

- International Conference on Metallurgical Coatings and Thin Films No31, San Diego, California, 2004, pp. 206–213.
- [20]- M.F. Doerner, W.D. Nix, A method for interpreting the data from depth-sensing indentation instruments. *J. Mater. Res.* 1(1986) 601–609. doi:10.1557/JMR.1986.0601
- [21]- J. Dunstan, Strain and strain relaxation in semiconductors, *J. Mater. Sci. Materials in Electronic* 8(6) (1997) 337–375. doi:10.1023/A:1018547625106
- [22]- S.C. Jain, A.H. Harker, R.A. Cowley, Misfit strain and misfit dislocations in lattice mismatched epitaxial layers and other systems, *Phil. Mag. A* 75; (1997) 1461–1515. doi:10.1080/01418619708223740
- [23]- F.C. Frank, W.T. Read Jr., In: *Proceedings of the Symposium on plastic deformation of crystalline solids*. Mellon Institute of Industrial Research, Pittsburgh U.S. Government Printing Office, 1950.
- [24]- S.V. Kamat, J.P. Hirth, Dislocation injection in strained multilayer structures, *J. Appl. Phys.* 67(1990) 6844. doi:10.1063/1.345074
- [25]- G.E. Beltz, L.B. Freund, On the Nucleation of Dislocations at a Crystal Surface. *Phys. Stat. Sol. B* 180(1993), 303–313.
- [26]- J.H. Van Der Merwe, Crystal Interfaces. Part II. Finite Overgrowths. *J. Appl. Phys.* 34(1963) 123. doi:10.1063/1.1729051
- [27]- J.W. Matthews, A.E. Blakeslee, Defects in epitaxial multilayers: I. Misfit dislocations. *J. Cryst. Growth*, 27(1974) 118–125. doi:10.1016/S0022-0248(74)80055-2